Self-Calibrating Microwave Characterization of Broadband Mach–Zehnder Electro-Optic Modulator Employing Low-Speed Photonic Down-Conversion Sampling and Low-Frequency Detection

Yangxue Ma, Zhiyao Zhang, Shangjian Zhang, Jun Yuan, Zhengping Zhang, Dongbing Fu, Jianan Wang, and Yong Liu

***Abstract*—An approach to characterizing the microwave performance of an electro-optic Mach–Zehnder modulator (MZM) is proposed based on photonic down-conversion sampling. Through low-speed sampling, the magnitude response of the MZM at the input microwave frequency is transferred to the duplicate component in the first Nyquist frequency range, and can be measured via low-frequency detection and spectrum analysis. A proof-of-concept experiment is carried out to demonstrate the feasibility of the proposed method, where magnitude-frequency response and half-wave voltage versus frequency of a commercial MZM in the frequency range of 0–40 GHz have been accurately measured under a sampling rate of 96.9 MS/s. Both simulation and experimental results indicate that the proposed method can be implemented without any extra calibration.**

***Index Terms*—Electrooptic modulators, frequency response, laser mode locking, microwave photonics.**

I. Introduction

MACH-ZENHDER electro-optic modulators, which are employed to impose electrical signals onto the intensity of light wave, are key components in the fields involving optical fiber communication [1], [2] and microwave photonics [3], [4]. In recent years, the bandwidth of the Mach-Zehnder modulator (MZM) has been enhanced to multi-tens of gigahertz or even hundreds of gigahertz, which has motivated various broadband applications such as microwave photonic mixer [5], [6], photonic analog-to-digital conversion [7], [8], and wideband tunable optoelectronic oscillator [9], [10]. For a broadband application, especially for a broadband microwave manipulation, the magnitude-frequency response (i.e., modulation depth at each frequency) of an MZM is critical for system performance, which is generally described by the half-wave voltage versus frequency [11]. Therefore, a precise measurement of the MZM half-wave voltage at each frequency is important for either performance optimization in the system design process or characteristic evaluation in the device manufacturing process.

Various methods have been brought forward to measure the microwave characteristic of the MZM. Based on the operation principle, the measuring techniques can be categorized into three groups, i.e., optical spectrum analysis method [12]–[14], electrical spectrum analysis method [15]–[20], and radio-frequency (RF) power analysis method [21]. The optical spectrum method is generally realized by monitoring the relative optical power between the carrier and the modulated sidebands through an optical spectrum analyzer (OSA). This method has tremendous advantage in the high-frequency region because of the large bandwidth of the OSA. However, the dynamic range over the low-frequency region and the start frequency of this method is usually limited by the spectral resolution of the commercially-available grating-based OSA which is generally 1.25 GHz (0.01 nm) @1550 nm. In addition, the dynamic range of the OSA is relatively small, which is not beneficial for measuring MZM with a bad microwave characteristic or under a small-signal modulation. One typical electrical method is based on the vector network analyzer (VNA) [18], [19], which is realized through loading the swept-frequency microwave signal onto the light wave via the MZM under test, and measuring the power gain of the corresponding microwave component recovered after a photodetector (PD). The frequency response could be measured precisely with a high frequency resolution through this method. However, the frequency response of the PD should be calibrated in this measurement, and the PD bandwidth must cover the frequency measurement range. Recently, another electrical method based on the so-called frequency-shifted heterodyne mixing is reported, where the frequency response can be calculated from the relative power of the two contiguous microwave signals

Manuscript received June 26, 2018; revised September 10, 2018; accepted October 5, 2018. Date of publication October 9, 2018; date of current version May 1, 2019. This work was supported in part by the National Natural Science Foundation of China under Grants 61575037 and 61421002, and in part by the Innovation Funds of Collaboration Innovation Center of Electronic Materials and Devices (ICEM2015-2001). *(Corresponding authors: Zhiyao Zhang and Jun Yuan.)*

Y. Ma, Z. Zhang, S. Zhang, and Y. Liu are with the State Key Laboratory of Electronic Thin Films and Integrated Devices, and the Collaboration Innovation Center of Electronic Materials and Devices, University of Electronic Science and Technology of China, Chengdu 610054, China (e-mail: mayangxue@126.com; zhangzhiyao@uestc.edu.cn; sjzhang@uestc.edu.cn; yongliu@uestc.edu.cn).

J. Yuan, Z. Zhang, D. Fu, and J. Wang are with the Science and Technology on Analog Integrated Circuit Laboratory, Chongqing 400060, China (e-mail: yjwlw@semi.ac.cn; lovezzpan@126.com; fudb@cetccq.com.cn; wangja1207@163.com).

Color versions of one or more of the figures in this paper are available online at http://ieeexplore.ieee.org.

Digital Object Identifier 10.1109/JLT.2018.2874965

acquired by the beating between the upper/lower modulated sideband and the frequency-shifted carrier in the PD [15]–[17]. In this method, the PD bandwidth requirement is only half of the frequency measurement range, and calibration of the PD frequency response is not needed. Nevertheless, for the measurement up to millimeter wave band, PD and electrical spectrum analyzer (ESA) with large bandwidths are still required. In order to relieve the bandwidth requirement of the PD, another electrical method based on low-frequency detection is proposed, which achieves MZM frequency response measurement by analyzing the low-frequency RF signals obtained through heterodyne beatings between the two-tone and bias-modulated optical signal [20]. Although this method accomplishes broadband MZM frequency response measurement via utilizing a low-speed PD, three microwave sources (i.e., a low-frequency one and the other two with bandwidths covering the frequency measurement range) are needed, which makes the measurement system complicated and expensive. The RF power analysis method employs an RF source and an RF power meter to achieve MZM measurement [21]. For a particular frequency, the half-wave voltage can be directly calculated from the input RF power which leads to a minimum output RF power from the PD. This method is extremely simple in its structure, and is free of PD response calibration. However, the bandwidth of the PD and the RF power meter must cover the frequency measurement range. In addition, to achieve half-wave voltage measurement at a single frequency, multiple measurements are required to determine the minimum-transmission point of the input/output RF power curve, which increases the measurement time.

In this paper, a self-calibrating method for measuring the half-wave voltage of a broadband MZM is proposed based on photonic down-conversion sampling and low-frequency detection. A passively mode-locked laser without any extra RF source is utilized to generate low-repetition-rate ultra-short optical pulse train. The pulse train samples a single swept-frequency microwave signal via the MZM under test, and the half-wave voltage of the MZM at each frequency can be calculated from the relative intensity between the Fourier frequency component in the first Nyquist frequency range and the direct current (DC) after PD. Both simulation and experiment are implemented to demonstrate the proposed scheme, where the measured half-wave voltages of a commercial MZM in a frequency range of 0–40 GHz employing the proposed method fit in with those measured through the two-tone method [17]. Compared with the method based on low-frequency detection in [20], only one microwave source is needed in the proposed method.

II. Operation Principle

The schematic diagram of the proposed broadband MZM microwave characterization method is shown in Fig. 1. The ultra-short optical pulse train from a passively mode-locked laser (MLL) is modulated by RF signal via the MZM under test. Then, the modulated optical pulse train is sent to a narrowband PD to obtain the low-frequency duplicate of the RF signal in the first Nyquist frequency range. At the output of the PD, an electrical spectral analyzer (ESA) is employed to acquire the

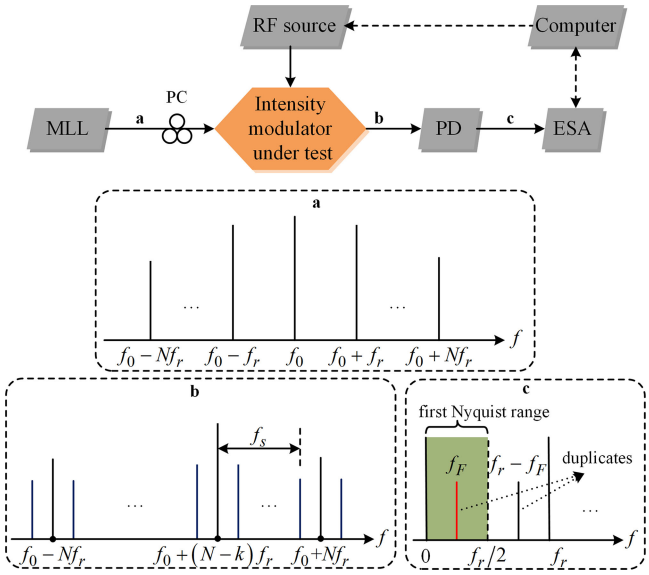

Fig. 1. Schematic diagram of the proposed MZM characterization method. MLL: mode-locked laser, PC: polarization controller, RF: radio-frequency, MZM: Mach-Zehnder modulator, PD: photodetector, ESA: electrical spectrum analyzer.

electrical spectrum. After that, the computer reads the spectrum information, and records the relative power of the low-frequency duplicate. So far, the magnitude response measurement at a single RF frequency is accomplished. The computer is also used to control the RF source to achieve frequency sweeping in the whole measurement range. The process described above is repeated until the magnitude response at each RF frequency has been measured. Finally, the half-wave voltage of the MZM is calculated from the measured magnitude response at each frequency. The detailed operation principle of the proposed broadband MZM microwave characterization scheme is described as follows.

Mathematically, for an MLL with a central frequency of and a repetition frequency of f_0 f_r, the output is a series of uniformly-spaced and equiform optical pulses, whose optical field can be expressed as

$$\begin{aligned} S_{MLL}(t) &= F_0 \sum_{l=-\infty}^{+\infty} p(t - l/f_r) \\ &= \sum_{n=-N}^{N} \left\{ p_n e^{j[2\pi(f_0 + n f_r)t]} + p_n e^{-j[2\pi(f_0 + n f_r)t]} \right\} \end{aligned} \tag{1}$$

where F_0 is the amplitude of the optical pulses, and $p(t)$ represents the time-domain envelope shape of a single optical pulse. p_n is the Fourier coefficient of $p(t)$, which represents the amplitude of the corresponding optical mode. N is an integer determined by the spectral width of the MLL. Then, a single-tone RF signal $v_{\text{in}}(t) = V\cos(2\pi f_s t)$ is made modulate the intensity of the optical pulse trains by the MZM under test, where f_s is an arbitrary RF frequency in the measurement range. For the MZM biased at the quadrature point, the output optical field after the

MZM can be written as

$$S_{MZM}(t) = S_{MLL}(t)\cos\left[\frac{\pi}{4} + \frac{m(f_s)}{2}\cos(2\pi f_s t)\right] \quad (2)$$

where $m(f_s)$ is the modulation index at the modulation frequency f_s, and can be calculated by

$$m(f_s) = \pi V / V_\pi(f_s) \quad (3)$$

where $V_\pi(f_s)$ is the half-wave voltage of the MZM at the modulation frequency f_s, and V is the voltage amplitude of the input RF signal. Then, the optical pulse sequence is sent to the PD where optical heterodyne beating occurs. The current from the PD can be written as

$$\begin{aligned} I_{PD}(t) &\propto R(f)\cdot S_{MZM}(t)\cdot S^*_{MZM}(t) \\ &= \sum_{n=-N}^{N}\sum_{l=-N}^{N} p_n p_l \cdot \left\{ \begin{array}{l} R[(n-l)f_r]\cos[2\pi(n-l)f_r t] \\ \quad +2R[(n-l)f_r \pm f_s]\, J_1[m(f_s)] \\ \quad \cdot\cos[2\pi(nf_r - lf_r \pm f_s)t] + \cdots \end{array} \right\} \end{aligned} \quad (4)$$

where $R(f)$ is the responsivity of the PD at the corresponding frequency f, and $J_1(x)$ is the first-order Bessel function of the first kind. As can be seen from (4), the input RF signal with a frequency of f_s has been copied to numerous duplicates. Since the MLL utilized here is a passively mode-locked fiber laser whose output pulses are ultra-short ones (generally with a pulse width of sub-picosecond, i.e., spectral width is multi- or multi-tens of nm), the number N is large enough to guarantee that there is always a frequency duplicate falling into the first Nyquist frequency range of $0 - f_r/2$. The frequency of the duplicate located in the first Nyquist frequency range is defined as Fourier frequency f_F, and can be written as

$$f_F = \begin{cases} f_s - kf_r & \mathrm{rem}(f_s/f_r) \le f_r/2 \\ kf_r - f_s & \mathrm{rem}(f_s/f_r) > f_r/2 \end{cases} \quad (5)$$

where $k = \mathrm{round}(f_s/f_r)$ is a natural number, denoting that f_s/f_r is rounded to the nearest integer. Additionally, $\mathrm{rem}(x)$ represents the remainder of x. The range of k is defined as $k \in [0, K]$ where K is a constant number determined by the max frequency of the input RF signal and the repetition frequency of the MLL. In general, K is much smaller than N, which is critically important for the approximation mentioned below. The repetition frequency of a passive MLL can be as low as tens of megahertz or below in practice, which makes the Fourier frequency lie in a small frequency range based on (5). Hence, it only needs a narrowband PD to detect the frequency duplicate. This condition is an important factor to guarantee the calibration-free of PD responsivity in the measurement.

The amplitude of the Fourier frequency component can be easily extracted from (4) as

$$i(f_F) = 2E_k R(f_F) J_1[m(f_s)] \quad (6)$$

where the coefficient E_k represents the contribution of the MLL spectral width and shape to the amplitude of the Fourier frequency component, and can be qualified as

$$E_k = 2\sum_{n=-N}^{N-k} p_n p_{n+k} \quad (7)$$

where the subscript k is determined by the relationship between the RF frequency f_s and the repetition frequency of MLL f_r as shown in (5). Additionally, the amplitude of direct current (DC) is

$$i(0) = E_0 R(0) \quad (8)$$

Therefore, the modulation index at an arbitrary RF frequency can be calculated through dividing the amplitude in (6) by that in (8) as

$$J_1[m(f_s)] = \frac{E_0 R(0)\, i(f_F)}{2E_k R(f_F)\, i(0)} \quad (9)$$

As mentioned above, K is generally much smaller than N when the optical pulse train employed to sample the RF signal is an ultra-short one. Hence, an approximation can be made as

$$E_0 \approx E_1 \approx E_2 \approx \cdots \approx E_K \quad (10)$$

In addition, if an MLL with a repetition frequency of tens of megahertz or below is employed in the measurement, the responsivity of the PD in the first Nyquist frequency range, i.e., $0 - f_r/2$, can be regarded to be identical. Hence, another approximation can be made as

$$R(0) \approx R(f_F) \quad (11)$$

Based on the above approximation, (9) can be simplified to be

$$J_1[m(f_s)] \approx \frac{i(f_F)}{2i(0)} \quad (12)$$

Therefore, $m(f_s)$, the modulation index at the modulation frequency f_s, can be directly calculated by the measured current at the Fourier frequency f_F and the DC component, which is free of calibration for both the PD responsivity and the MLL spectrum. Finally, the half-wave voltage of the MZM at each RF frequency can be calculated from the measured modulation index $m(f_s)$ based on (3). So far, the microwave characteristic measurement is accomplished.

If the frequency measurement range is not much smaller than the spectral bandwidth of the MLL, (10) is not valid any more. In this situation, the influence of the MLL spectrum (denoting by $E_k, k = 0, 1, \ldots K$) on the measurement accuracy must be considered, and be removed to guarantee an accurate measurement result. A compensatory process is therefore proposed to quantitatively acquire the influence of E_k $(k = 0, 1, \ldots K)$ in the measurement, which is realized by employing two RF signals with frequencies of $f_1 = f_r/2 - \Delta f$ and $f_2 = f_r/2 + \Delta f$ (Δf is a very small frequency) to modulate the MZM separately. According to the down-conversion sampling theory, Fourier frequency is identical for the two input RF signals. The corresponding current from the PD for the two input RF signals can be expressed

respectively as

$$\begin{aligned} I_1(t) \propto & \sum_k E_k R(kf_r)\cos(2\pi k f_r t) \\ & + 2E_0 R(f_r/2-\Delta f) J_1[m(f_1)] \cos[2\pi(f_r/2-\Delta f)t] \\ & + 2E_1 R(f_r/2+\Delta f) J_1[m(f_1)] \cos[2\pi(f_r/2+\Delta f)t] \\ & + 2E_1 R(3f_r/2-\Delta f) J_1[m(f_1)] \cos[2\pi(3f_r/2-\Delta f)t] \\ & + 2E_2 R(3f_r/2+\Delta f) J_1[m(f_1)] \cos[2\pi(3f_r/2+\Delta f)t] \\ & + \cdots \end{aligned} \tag{13a}$$

$$\begin{aligned} I_2(t) \propto & \sum_k E_k R(kf_r)\cos(2\pi k f_r t) \\ & + 2E_1 R(f_r/2-\Delta f) J_1[m(f_2)] \cos[2\pi(f_r/2-\Delta f)t] \\ & + 2E_1 R(f_r/2+\Delta f) J_1[m(f_2)] \cos[2\pi(f_r/2+\Delta f)t] \\ & + 2E_2 R(3f_r/2-\Delta f) J_1[m(f_2)] \cos[2\pi(3f_r/2-\Delta f)t] \\ & + 2E_2 R(3f_r/2+\Delta f) J_1[m(f_2)] \cos[2\pi(3f_r/2+\Delta f)t] \\ & + \cdots \end{aligned} \tag{13b}$$

Through employing an ESA to measure the two currents given in (13a) and (13b), it is easy to quantify the amplitudes corresponding to the duplicates of f_1 in each Nyquist frequency range as

$$\begin{aligned} i_1(f_r/2-\Delta f) &= 2E_0 R(f_r/2-\Delta f) J_1[m(f_1)] \\ i_1(f_r/2+\Delta f) &= 2E_1 R(f_r/2+\Delta f) J_1[m(f_1)] \\ i_1(3f_r/2-\Delta f) &= 2E_1 R(3f_r/2-\Delta f) J_1[m(f_1)] \\ &\cdots \end{aligned} \tag{14}$$

and the amplitudes corresponding to the duplicates of f_2 as

$$\begin{aligned} i_2(f_r/2-\Delta f) &= 2E_1 R(f_r/2-\Delta f) J_1[m(f_2)] \\ i_2(f_r/2+\Delta f) &= 2E_1 R(f_r/2+\Delta f) J_1[m(f_2)] \\ i_2(3f_r/2-\Delta f) &= 2E_2 R(3f_r/2-\Delta f) J_1[m(f_2)] \\ &\cdots \end{aligned} \tag{15}$$

Therefore, the ratio of E_{k+1} to E_k $(k=0,1,\ldots K)$ can be calculated as

$$\frac{E_{k+1}}{E_k} = \frac{i_1[(2k+1)f_r/2+\Delta f]}{i_1[(2k+1)f_r/2-\Delta f]} \cdot \frac{i_2[(2k+1)f_r/2-\Delta f]}{i_2[(2k+1)f_r/2+\Delta f]} \tag{16}$$

which is absolutely independent of the PD responsivity and the MZM frequency response. Finally, (12), which is used to calculate the modulation index at the modulation frequency, is redefined as

$$J_1[m(f_s)] = \frac{i(f_F)}{2i(0)} \frac{E_{k-1}}{E_k} \frac{E_{k-2}}{E_{k-1}} \cdots \frac{E_0}{E_1} \tag{17}$$

It should be pointed out that, if the influence of the MLL spectrum is required to be removed in the measurement based on (13)–(17), a PD with a broad bandwidth and an ESA with a large frequency measurement range are needed, which inevitably increases the complexity and cost of the measurement setup. Fortunately, since the spectral width of the passive MLL is generally much larger than the frequency measurement range, the error caused by the approximation of E_k based on (10) is tiny, which can be neglected without losing measurement accuracy. Therefore, it only needs a PD with a narrow bandwidth and an ESA with a small frequency measurement range to measure the frequency response of the MZM based on (12).

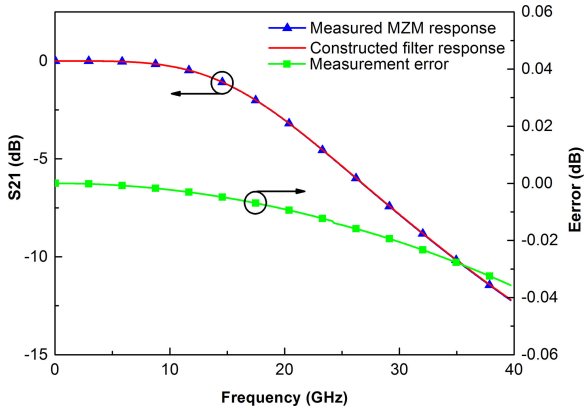

Fig. 2. Simulated MZM frequency response and measurement error.

III. Simulation and Analysis

In this section, numerical simulation is implemented to evaluate the performance of the proposed microwave characterization approach. The repetition frequency and the full width at half maximum (FWHM) of the hyperbolic-secant-shaped optical pulses from the MLL are set to be 97 MHz and 1 ps, respectively. Hence, the corresponding 3-dB spectral width of the MLL is 3.8 nm in the simulation, which would introduce a larger measurement error than that employing a real passive MLL (generally with a pulse width of sub-picosecond) caused by the approximation of (10). The frequency responses of both the MZM and the PD in the simulation are imitated by 2nd-order Butterworth filter, where the 3-dB bandwidths of the MZM and the PD are set to be 20 GHz and 3 GHz, respectively.

Firstly, microwave characterization of the MZM in the frequency range of 0–40 GHz is carried out based on (12). The input RF signal is swept from 25 MHz to 39989 MHz with a step of 97 MHz to guarantee that Fourier frequency after PD is located at 25 MHz for each input RF signal. Fig. 2 presents the simulated frequency response and measurement error, where the red solid line, the blue triangle solid line and the green square solid line represent the constructed filter response (2nd-order Butterworth filter with a 3-dB bandwidth of 20 GHz), the measured MZM response and the measurement error, respectively. It should be pointed out that the measurement error here is a relative error, which is defined in percent as $[(\text{measured value} - \text{true value})/\text{true value}]$, and is denoted in decibel as relative error$(dB) = 10^* \log(\text{relative error}(\%) + 1)$.

As can be seen in Fig. 2, the measured frequency response fits in with the preset filter response, which indicates that the proposed scheme can be utilized to measure the MZM frequency

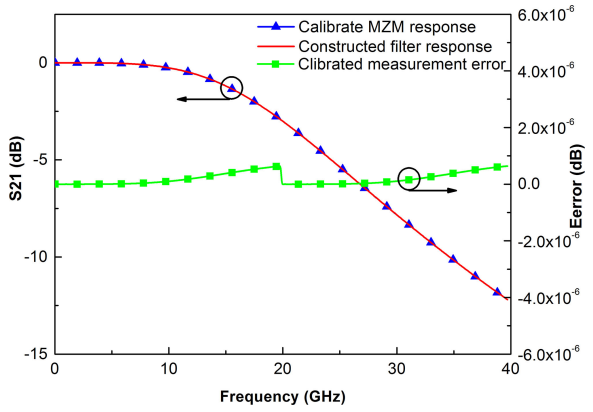

Fig. 3. Calibrated MZM frequency response and corresponding measurement error.

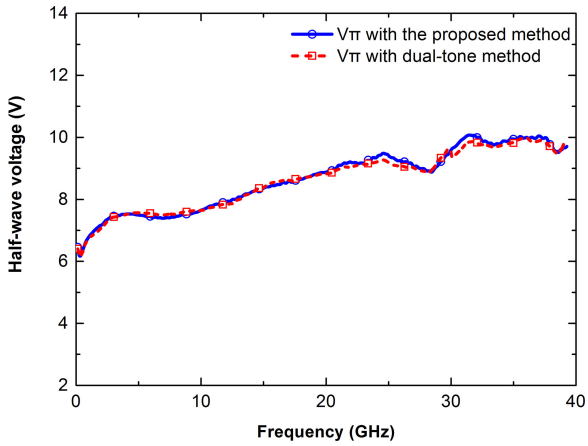

Fig. 4. Measured half-wave voltages of the MZM versus frequency.

response accurately. It can be also seen from Fig. 2 that the measurement error increases with the RF frequency, where the largest measurement error in the frequency range of 0–40 GHz is 0.035 dB. This tolerable measurement error is introduced by the approximation shown in (10), and it can be further reduced by employing an MLL with a narrower pulse width (i.e., a broader spectral width).

Then, (17) is used to eliminate the influence of the MLL spectrum on the measurement result. In order to obtain the ratio of E_{k+1} to E_k $((k = 0, 1, \ldots K))$, two RF signals with frequencies of 48 MHz and 49 MHz (corresponding to $\Delta f = 0.5$ MHz) are employed to modulate the optical pulse train via the MZM separately. Additionally, the 3-dB bandwidth of the PD is reset to be 16 GHz. Through acquiring the electrical spectra after the PD under the above-mentioned two input RF signals, the ratio of E_{k+1} to E_k $(k = 0, 1, \ldots K)$ is calculated based on (16), and is employed to eliminate the influence of the MLL spectrum on the measurement result based on (17). Fig. 3 exhibits the calibrated frequency response and the corresponding measurement error. It can be seen that the maximum measurement error in the frequency range of 0–40 GHz is reduced to 1×10^{-6} dB after removing out the influence of the MLL spectrum, which again indicates that the measurement error in Fig. 2 is induced by the MLL with a relatively narrow spectral width employed in the simulation. Furthermore, it should be pointed out that the calibration of E_k approximation is unnecessary since the measurement error is far below the measurement accuracy of a commercial ESA.

Finally, it should be noted that the frequency response of an actual MZM is complex, and cannot be simply represented by a basic filter function (including the 2nd-order Butterworth filter). The selection of a 2nd-order Butterworth filter with a 3-dB bandwidth of 20 GHz in the simulation is merely an example to visualize the measurement error of the proposed method. The results employing other digital filters with different shapes, orders and even bandwidth lead to the same conclusion. Therefore, it can be summarized that, if the spectral width of the MLL is much larger than the frequency measurement range (more than ten times), the measurement error induced by the optical spectrum is negligible even without a calibration.

IV. Experimental Results and Discussion

A proof-of-concept experiment is carried out to demonstrate the proposed approach. In the experiment, a passively mode-locked erbium-doped fiber laser (Calmar FPL-02CFF) with a repetition frequency of 96.9 MHz, a central wavelength of 1550.2 nm and a 3-dB spectral width of 11.1 nm is employed as the light source. The test sample is a commercial MZM (EOSPACE AX-OMSS-20), which is biased at its quadrature point in the experiment. The optical pulse sequence generated by the MLL is sent to the MZM via a polarization controller, and is modulated by the RF signals from a microwave source (R&S SMB 100 A). The microwave source is controlled by a computer to sweep its output frequency from 25 MHz to 39754 MHz with a step of 96.9 MHz. Then, the modulated pulse train is sent to a PD (HP 11982A) to achieve optical heterodyne beating, and the output electrical signal is measured by an ESA (R&S FSU50). The spectrum data under each input RF signal frequency is recorded by the computer, in which the power data of the useful frequency components are selected and stored. Finally, the half-wave voltage at each RF signal frequency and the magnitude-frequency response of the MZM are calculated using the measured data. In order to demonstrate the validation of the measurement result utilizing the proposed approach, another experiment using the heterodyne-mixing-based dual-tone microwave characterization scheme proposed in [17] is also implemented as a comparison. The accuracy of this dual-tone method has already been demonstrated through comparing its measurement results with those using the optical spectrum analysis method, and its schematic diagram can be found in [17].

Fig. 4 and Fig. 5 show the measured half-wave voltage versus frequency and the magnitude-frequency response, respectively, where the blue solid line with open circles represents the measurement result using the proposed method, and the red dashed line with open squares denotes that using the dual-tone method. Thereinto, the S_{21} curve is obtained through calculating the decibel of the normalized reciprocal of the half-wave voltage. The good match between the two measurement results indicate that the proposed method can be utilized to accurately measure the microwave characteristic of the MZM.

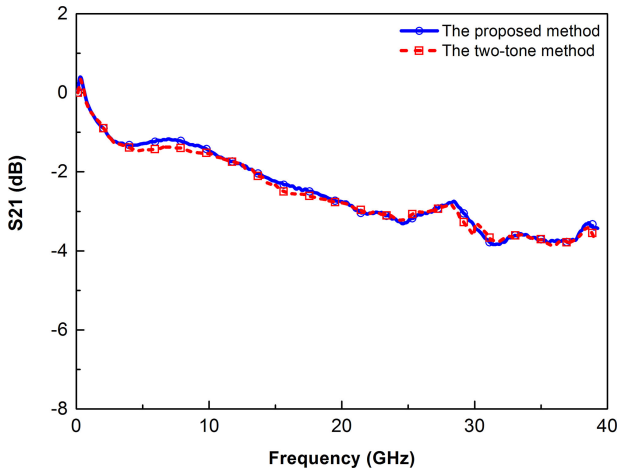

Fig. 5. Measured magnitude-frequency response of the MZM.

Since there is no exact value of the MZM frequency response for reference in the experiment, precise measurement error cannot be obtained. The measurement error in the experiment can be evaluated as follows. Firstly, it should be pointed out that the calculation of modulation index $m(f_s)$ in the experiment is slightly different from that given in (12). Since the amplitude of the DC current cannot be measured by the ESA with alternating current (AC) coupling in the experiment, $i(0)$ in (12) is substituted by the amplitude of the current at the frequency of f_r as

$$i(f_r) = E_1 R(f_r) \tag{18}$$

This substitution is valid since the difference between $i(0)$ and amplitude of the current at DC, f_r, $2f_r$ and $3f_r$ is different only below the fourth bits after the decimal point (with an unit of dB), which indicates that the current amplitude difference between the DC component and the f_r component has a negligible influence on the measurement accuracy. In the experiment, the power at f_r, $2f_r$ and $3f_r$ is measured to be -11.42 dBm, -11.38 dBm and -11.49 dBm, where the power difference is mainly attributed to the power measurement uncertainty of the ESA (less than 0.1 dB based on the specification). Finally, it can be concluded that there are two reasons for the small discrepancy between the measurement result using the proposed approach and that using the two-tone method. The first one is attributed to the power measurement uncertainty of the frequency components f_F and f_r by the ESA, which introduce a measurement error in the range of ± 0.2 dB. The other one is attributed to the approximation of E_k as given in (10), which is expected to be less than 0.035 dB in the experiment, and much smaller than that induced by the power measurement uncertainty of the ESA. Therefore, the influence of the MLL spectrum on the measurement result is unnecessary to remove in the experiment, which makes the proposed measurement approach calibration-free of the approximation of E_k.

It should be pointed out that the half-wave voltage is proportional to the operation wavelength according to the theory of electro-optic modulation based on Pockel effect [22]. Therefore, the measured half-wave voltage is an average in the MLL wavelength range. For the MLL operating in 1550 nm wavelength range, the variation of half-wave voltage is less than $\pm 0.6\%$ in a wavelength range of ± 10 nm $(10/1550 = 0.006)$, which is smaller than the ESA-induced measurement error of ± 0.2 dB ($\pm 2.3\%$). Moreover, since the spectrum of the MLL is symmetrical around the central wavelength, the half-wave voltage deviation due to wavelength difference is counteracted. Therefore, the measured half-wave voltage is considered as the half-wave voltage at the central wavelength of the MLL. If the half-wave voltages at different wavelengths are required, a wavelength tunable MLL can be utilized [23].

Furthermore, the noise floor is measured to be -100 dBm in the experiment with a resolution bandwidth (RBW) of 2 kHz. Considering that the maximum measurable power of the ESA is 30 dBm, the dynamic range of the measurement setup is 130 dB@2 kHz. The highest RBW of the ESA employed in the experiment is 10 Hz. Hence, the dynamic range of the measurement setup can be as larger as 153 dB.

It should be noticed that the proposed method can only be used to measure the microwave characteristic of the electro-optic intensity modulators (such as MZM), and is not feasible for phase modulator (PM) characterization. In the proposed method, the half-wave voltage of an MZM is obtained from the relative intensity between the Fourier frequency component and the DC one. Since phase modulation has no influence on the RF spectrum after the PD, no RF component (such as the Fourier frequency component) that carries the magnitude response of the PM is generated. Hence, the proposed method cannot be directly applied to measure the microwave characteristic of the PM in principle. In order to use the proposed method to achieve PM characterization, extra phase modulation to intensity modulation conversion must be added before photodetection.

Finally, it should be noted that the light source utilized in the experiment is a passive MLL with a low repetition frequency, which is also a kind of optical frequency comb (OFC). Therefore, the MLL in the proposed method can be replaced by other OFC sources which have the following three characteristics. The first one is that the combs should be phase-locked, which guarantees that the RF signals with identical frequency generated by the beating between different combs and the modulation sidebands do not cancel out each other. The second one is that the spectral width should be much larger than the frequency measurement range, which guarantees that the error caused by the approximation in (10) is negligible. The third one is that frequency spacing should be small, which guarantees that the measurement system is a low-frequency detection one and the PD response is uniform in the first Nyquist range.

V. Conclusion

In conclusion, we have presented and experimentally demonstrated an approach to characterize the microwave performance of MZMs based on low-speed photonic down-conversion sampling and low-frequency detection. Through using the proposed method, magnitude-frequency response and half-wave voltage versus frequency of a commercial MZM in the frequency range of 0–40 GHz have been accurately measured via employing a

passively mode-locked erbium-doped fiber laser with a repetition frequency of 96.9 MHz, which fit in with those measured through the two-tone method [17]. Both simulation and experimental results indicate that the proposed method can be implemented without any extra calibration procedure. The main advantage of the proposed method is that it only needs a single microwave source in the measurement, which greatly reduce the measurement setup complexity and cost compared with the existing method based on low-detection in [20]. In addition, due to the large bandwidth of the passive MLL employed in the experimental setup (generally greater than several hundred GHz), the frequency measurement range can be easily extended to hundreds of GHz by using a microwave source with a bandwidth covering the frequency measurement range.

REFERENCES

[1] X. Pang *et al.*, "100 Gbit/s hybrid optical fiber-wireless link in the W-band (75-110 GHz)," *Opt. Express*, vol. 19, no. 25, pp, 24944–24949, Nov. 2011.

[2] D. Zibar *et al.*, "High-capacity wireless signal generation and demodulation in 75- to 110-GHz band employing all-optical OFDM," *IEEE Photon. Technol. Lett.*, vol. 23, no. 12, pp. 810–812, Jun. 2011.

[3] J. Capmany and D. Novak, "Microwave photonics combines two worlds," *Nature Photon.*, vol. 1, no. 6, pp. 319–330, Jun. 2007.

[4] J. Yao, "Microwave photonics," *J. Lightw. Technol.*, vol. 24, no. 12, pp. 4628–4641, Feb. 2009.

[5] Z. Tang and S. Pan, "Reconfigurable microwave photonic mixer with minimized path separation and large suppression of mixing spurs," *Opt. Lett.*, vol. 42, no. 1, pp. 33–36, Jan. 2017.

[6] X. Zou *et al.*, "Microwave photonic harmonic down-conversion based on cascaded four-wave mixing in a semiconductor optical amplifier," *IEEE Photon. J.*, vol. 10, no. 1, Feb. 2018, Art. no. 5500308.

[7] D. J. Esman *et al.*, "Highly linear broadband photonic-assisted Q-band ADC," *J. Lightw. Technol.*, vol. 33, no. 11, pp. 2256–2262 Jun. 2015.

[8] J. Mallari *et al.*, "100 Gbps EO polymer modulator product and its characterization using a real-time digitizer," in *Proc. Opt. Fiber Commun. Conf. Exhib.*, Mar. 2010, Paper OThU.2.

[9] C. Li *et al.*, "Widely tunable optoelectronic oscillator using a dispersion-induced single bandpass MPF," *IEEE Photon. Technol. Lett.*, vol. 30, no. 1, pp. 7–10, Jan. 2018.

[10] H. Peng *et al.*, "Tunable DC-40 GHz RF generation with high side-mode suppression utilizing a dual loop Brillouin optoelectronic oscillator," in *Proc. Opt. Fiber Commun. Conf. Exhib.*, Mar. 2015, Paper M3E.5.

[11] F. Heismann, S. K. Korotky, and J. J. Veselka, "Lithium niobate integrated optics: Selected contemporary devices and system applications," in *Optical Fiber Telecommunications IIIb*. New York, NY, USA: Lucent Technologies, 1997, pp. 377–462.

[12] S. Oikawa, T. Kawanishi, and M. Izutsu, "Measurement of chirp parameters and halfwave voltages of Mach-Zehnder-type optical modulators by using a small signal operation," *IEEE Photon. Technol. Lett.*, vol. 15, no. 5, pp. 682–684, May 2003.

[13] Y. Shi, L. Yan, and A. E. Willner, "High-speed electrooptic modulator characterization using optical spectrum analysis," *J. Lightw. Technol.*, vol. 21, no. 10, pp. 2358–2367, Oct. 2003.

[14] Y. Liao, H. Zhou, and Z. Meng, "Modulation efficiency of a $LiNbO_3$ waveguide electro-optic intensity modulator operating at high microwave frequency," *Opt. Lett.*, vol. 34, no. 12, pp. 1822–1824, Jun. 2009.

[15] S. Zhang *et al.*, "Calibration-free electrical spectrum analysis for microwave characterization of optical phase modulators using frequency-shifted heterodyning," *IEEE Photon. J.*, vol. 6, no. 4, Aug. 2014, Art. no. 5501008.

[16] H. Wang *et al.*, "Self-calibrated and extinction-ratio-independent microwave characterization of electrooptic Mach-Zehnder modulators," *IEEE Microw. Wireless Compon. Lett.*, vol. 27, no. 99, pp. 948–950, Oct. 2017.

[17] H. Wang *et al.*, "Calibration-free and bias-drift-free microwave characterization of dual-drive Mach–Zehnder modulators using heterodyne mixing," *Opt. Eng.*, vol. 55, no. 3, p. 031109, Mar. 2015.

[18] M. Xue, Y. Heng, Y. Heng, and S. Pan, "Ultrahigh-resolution electro-optic vector analysis for characterization of high-speed electro-optic phase modulators," *J. Lightw. Technol.*, vol. 36, no. 9, pp. 1644–1649, May 2018.

[19] P. D. Hale and D. F. Williams, "Calibrated measurement of optoelectronic frequency response," *IEEE Trans. Microw. Theory Techn.*, vol. 51, no. 4, pp. 1422–1429, Apr. 2003.

[20] S. Zhang *et al.*, "Calibration-free measurement of high-speed Mach-Zehnder modulator based on low-frequency detection," *Opt. Lett.*, vol. 41, no. 3, pp. 460–463, Feb. 2016.

[21] H. V. Roussell and E. I. Ackerman, "Method and apparatus for determining frequency-dependent Vπ of a Mach-Zehnder optical modulator," U.S. Patent 7 760 343 B2, Jul. 20, 2010.

[22] R. G. Hunsperger, "Electro-optics modulator," in *Integrated Optics: Theory and Technology*, 6th ed. Berlin, Germany: Springer Science+Business Media, 2009, pp. 108–125.

[23] F. Wang *et al.*, "Wideband-tuneable, nanotube mode-locked, fibre laser," *Nature Nanotechnol.*, vol. 3, no. 12, pp. 738–42, Dec. 2008.

Yangxue Ma received the B.S. degree in electronic science and technology, in 2012, from the University of Electronic Science and Technology of China, Chengdu, China, where she is currently working toward the Ph.D. degree in optical engineering. Her research interests include photonic analog-to-digital conversion and microwave photonics mixing.

Zhiyao Zhang received the B.S. degree in electronic science and technology and the Ph.D. degree in optical engineering from the University of Electronic Science and Technology of China, Chengdu, China, in 2005 and 2010, respectively. In 2010, he joined the University of Electronic Science and Technology of China as a Lecturer, where he became an Associate Professor in 2014. In 2017, he was a Visiting Scholar with the Microwave Photonics Research Laboratory, School of Electrical Engineering and Computer Science, University of Ottawa, ON, Canada. His current research interests include microwave photonics and nonlinear fiber optics.

Shangjian Zhang received the B.S. and M.S. degrees from the University of Electronic Science and Technology of China, Chengdu, China, in 2000 and 2003, respectively, and the Ph.D. degree from the Institute of Semiconductors, Chinese Academy of Sciences, Beijing, China, in 2006. He was a Visiting Researcher with the COBRA Research Institute, Eindhoven University of Technology, Eindhoven, The Netherlands. He is currently a Professor with the University of Electronic Science and Technology of China. In 2016 to 2017, he was on sabbatical with the University of California, Santa Barbara, CA, USA. He has authored or coauthored more than 100 papers and holds seven patents. His research interests include high-speed optoelectronic devices and photonic microwave signal processing.

Jun Yuan, biography not available at the time of publication.

Zhengping Zhang, biography not available at the time of publication.

Dongbing Fu, biography not available at the time of publication.

Jianan Wang, biography not available at the time of publication.

Yong Liu received the master's degree from the University of Electronic Science and Technology of China, Chengdu, China, in 1994, and the Ph.D. degree from Eindhoven University of Technology, Eindhoven, The Netherlands, in 2004. From 1994 to April 2000, he was with the University of Electronic Science and Technology of China. In April 2000, he joined the COBRA Research Institute, Eindhoven University of Technology. Since 2007, he has been a Professor with the University of Electronic Science and Technology of China. He has (co)authored more than 200 journal and conference papers. His research interests include optical nonlinearities and applications, optical signal processing, and optical fiber technologies. He received the Chinese National Science Fund for Distinguished Young Scholars in 2009 and Chinese Chang Jiang Scholar in 2013. He received an IEEE Lasers and Electro-Optics Society Graduate Student Fellowship in 2003.